Enabling Joint Radar-Communication Operation in Shift Register-Based PMCW Radars

Lucas Giroto de Oliveira*, Elizabeth Bekker, Axel Diewald, Benjamin Nuss,
Theresa Antes, Yueheng Li, Akanksha Bhutani, and Thomas Zwick
Institute of Radio Frequency Engineering and Electronics (IHE)
Karlsruhe Institute of Technology (KIT), Germany
E-mail: *lucas.oliveira@kit.edu

Abstract—**This article introduces adaptations to the conventional frame structure in binary phase-modulated continuous wave (PMCW) radars with sequence generation via linear-feedbck shift registers and additional processing steps to enable joint radar-communication (RadCom) operation. In this context, a preamble structure based on pseudorandom binary sequences (PRBSs) that is compatible with existing synchronization algorithms is outlined, and the allocation of pilot PRBS blocks is discussed. Finally, results from proof-of-concept measurements are presented to illustrate the effects of the choice of system and signal parameters and validate the investigated PMCW-based RadCom system and synchronization strategy.**

Index Terms—**Phase-modulated continuous wave (PMCW), pseudorandom binary sequence (PRBS), joint radar-communication (RadCom), synchronization.**

I. INTRODUCTION

Due to its low linearity requirements and high performance as a modulation scheme for fully digital radar systems, binary phase-modulated continuous wave (PMCW) has continuously gained interest for highly automated driving (HAD) applications. In this context, using linear-feedback shift registers (LFSRs) instead of digital-to-analog converters (DACs) to generate transmit pseudorandom binary sequences (PRBSs) appears as an efficient approach to achieve a simplified transmitter architecture while keeping a robust radar performance [1]. With minor adaptations to the PMCW transmitter [2], joint radar-communication (RadCom) operation with the transmission of binary phase-shift keying (BPSK) symbols as described in [3] is also possible. This results in high communication robustness due to the experienced processing gain from accumulation and correlation, but in rather low data rates. The latter are, however, sufficient for radar-centric operation of the PMCW-based RadCom system, in which basic control information is exchanged and tasks such as interference cancellation (IC) are performed [4].

In this article, a design of binary preambles for synchronization is proposed and a pilot arrangement for channel, Doppler shift, and residual sampling frequency offset (SFO) estimation is discussed for the considered PMCW-based RadCom system. Proof-of-concept measurement results are finally presented to validate the proposed synchronization strategy.

II. SYSTEM MODEL

Let a single-input single-output (SISO) PMCW-based radar system be based on the transmission of a PRBS of length $N \in \mathbb{N}_{>0}$. More specifically, an m-sequence, also known as maximum-length sequence (MLS), is used, which results in $N = 2^m - 1 | m \in \mathbb{N}_{\geq 2}$. Every set of $A \in \mathbb{N}_{>0}$ identical PRBSs constitutes a block, which is evaluated at the receiver side to yield a range profile. This is achieved by (i) discarding the first PRBS within the block at the receiver side, letting it act as a cyclic prefix (CP), (i) accumulating the remaining $A - 1$ PRBSs repetitions, and (iii) performing a circular correlation between the resulting N-length accumulated PRBS and the originally transmitted reference PRBS. With the transmission of a frame containing $M \in \mathbb{N}_{>0}$ blocks, discrete Fourier transforms (DFTs) can be performed along the bins of the range profiles to estimate Doppler shifts and ultimately generate a range-velocity radar image.

To enable RadCom operation of such PMCW-based radar system while still transmitting only binary sequences, each of the M blocks in the PMCW frame is modulated with a single BPSK symbol [3], [5]. At the receiver side, of another PMCW-based RadCom system, the same processing encompassing accumulation and circular correlation with the reference PRBS as in the radar case is performed. After equalization, this results in M blocks containing the autocorrelation of the reference PRBS modulated by the corresponding BPSK symbols, which can be extracted from the autocorrelation peak since it experiences the most processing gain, i.e., $N(A - 1)$ [3].

At the transmitter side of the considered PMCW-based RadCom system, the NAM PRBSs in the transmit frame are generated by a single LFSR with sampling rate F_s and then BPSK-modulated. The discrete-time domain sequence output by the modulator is denoted by $x[n] \in \mathbb{C}$, $n \in \mathbb{Z}$ and has an equivalent continuous-time domain baseband transmit signal $x(t) \in \mathbb{C}$. Besides undergoing analog conditioning, e. g., to filter out out-of-band (OOB) emission, $x(t) \in \mathbb{C}$ is upconverted to the carrier frequency $f_\mathrm{c} \gg B$ and radiated by the transmit antenna. The aforementioned signal propagates through the medium and is eventually received by the receive antenna of a second PMCW-based RadCom system. The receive signal is then conditioned and downconverted to the baseband in an I/Q analog front-end (AFE), resulting in the continuous-time domain signal without noise $\tilde{y}(t) \in \mathbb{C}$. It is henceforth assumed that $\tilde{y}(t)$ is the result of the propagation of $x(t)$ through a stronger, main path and multiple secondary paths, each with own delay, Doppler shift and phase rotation.

Additionally, $\tilde{y}(t)$ contains the effects of mismatches between the transmitting and the receiving PMCW-based RadCom systems. Those are symbol time offset (STO) due to distinct time references, besides carrier frequency offset (CFO) and its resulting carrier phase offset (CPO) raised by the use of distinct oscillators by the non-collocated transmitter and receiver pair. To generate a discrete-time domain receive sequence $y[n] \in \mathbb{C}$ at the receiver side, the noise-impaired version of $\tilde{y}(t)$ undergoes analog-to-digital (A/D) conversion with a sampling rate set to the same value as at the transmitter, i.e., F_s. However, as the sampling clock at the receiver is asynchronous w.r.t. the one at the transmitter, SFO occurs.

To extract BPSK data from $y[n]$, one must perform (i) synchronization to compensate for CFO, STO, and SFO, (ii) compensation of Doppler shifts, and (iii) channel estimation and equalization to compensate for multipath propagation. The aforementioned task (i) can be performed via processing based on the transmission of a known preamble. After synchronization, a receive PMCW frame can be formed and the last $A-1$ PRBSs of each block accumulated. The resulting blocks can be then circularly correlated with the reference PRBS, and channel response and Doppler shift estimates can be obtained from the pilot blocks. Finally, tasks (ii) and (iii) are performed, i.e., both Doppler shift and channel frequency response (CFR) are compensated, and the receive BPSK symbols are extracted from the non-pilot or payload (PL) blocks.

III. Preamble Design and Pilot Arrangement

In this article, a preamble is designed to meet requirements of both the Schmidl & Cox (S&C) [6] (for time and frequency synchronization) and the Tsai [7] (for sampling frequency synchronization) algorithms typically used in orthogonal frequency-division multiplexing (OFDM)-based systems, while equally-spaced, reserved blocks modulated with known BPSK symbols at the receiver are used as pilots. To keep the transmitter architecture simple and linearity requirements low, both the preamble and pilots are required to be binary. The design of a binary preamble that meets the requirements of the adopted synchronization algorithms and the arrangement of pilots are discussed in Sections III-A and III-B, respectively.

A. Binary Preamble Design

To perform time and frequency synchronization in the considered PMCW-based RadCom system, compensating both STO and CFO, $M_{\text{S\&C}} = 2$ binary preamble blocks that meet the requirements of the S&C algorithm are used [6]. Additionally, a sequence of $M_{\text{SFO}} \in \mathbb{N}_{>0}$ PRBSs is designed to meet the requirements of the Tsai algorithm for SFO estimation. Their design requirements is discussed as follows.

1) Preamble Blocks for Schmidl & Cox Algorithm: For the S&C algorithm, a preamble containing $M_{\text{S\&C}} = 2$ blocks of length $N_{\text{block}}^{\text{S\&C}} \in \mathbb{N}_{>0}$ is necessary. Disregarding CP, one typically adopts $N_{\text{block}}^{\text{S\&C}} = N$ in OFDM systems and designs the first block so that it consists of two equal halves, which results in a discrete-frequency domain spectrum with interleaved active tones. The second block must be designed
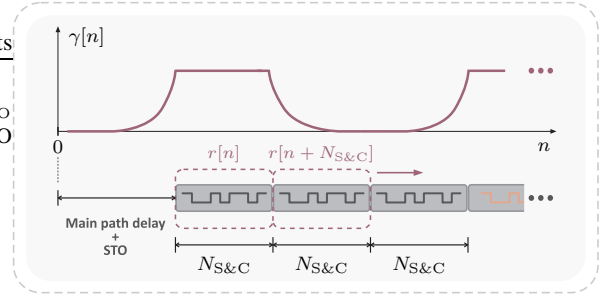

Fig. 1. Sliding window correlation and PRBS-based S&C preamble.

so that at least the same tones as in the first preamble block are active, although usually all tones are active for OFDM.

It is henceforth assumed that the length $N_{\text{block}}^{\text{S\&C}}$ of the two preamble blocks used for the S&C algorithm is $N_{\text{block}}^{\text{S\&C}} = 3N_{\text{S\&C}}$, where $N_{\text{S\&C}} \in \mathbb{N}_{>0}$ is the length of a PRBS such that $N_{\text{S\&C}} = \lceil (N+1)/2 \rceil - 1$. In other words, each preamble block is composed of three repetitions of an MLS whose length is approximately the half of the PL PRBS length N. The first repetition acts as a CP, while the latter two are the required equal halves for the S&C algorithm. Although these equal halves are only indispensable for the first S&C block, the same structure is kept for the second one to keep the same block length as the PRBS lengths are not flexible. The use of the considered preamble allows to find the start point of the PMCW frame at the receiver via a sliding-window correlation. As illustrated in Fig. 1, a correlation-like processing is performed between two sliding windows of length $N_{\text{S\&C}}$ starting at the reference sample n from $y[n]$, namely $r[n]$ and $r[n + N_{\text{S\&C}}]$. The result is expressed as

$$\gamma[n] = \frac{\left| \sum_{\eta=0}^{N_{\text{S\&C}}-1} r^*[n+\eta] r[n+\eta+N_{\text{S\&C}}] \right|^2}{\sum_{\eta=0}^{N_{\text{S\&C}}-1} |r[n+\eta+N_{\text{S\&C}}]|^2}. \quad (1)$$

Assuming orthogonal PRBSs for each S&C preamble block, which requires distinct LFSRs, $\gamma[n]$ will present two spaced plateaus of length $N_{\text{S\&C}}$, each associated with one of the S&C preamble blocks. Considering only the first plateau, the frame start point can be estimated as one of the sample positions within the plateau [6]. Additionally, the phase of the term $\sum_{\eta=0}^{N_{\text{S\&C}}-1} r^*[n+\eta] r[n+\eta+N_{\text{S\&C}}]$ in the numerator of $\gamma[n]$ can be evaluated to estimate the fractional CFO (non-integer multiple of $F_s/(2N_{\text{S\&C}})$), and the first and second preamble blocks can be compared to estimate the integer CFO (integer multiple of $F_s/(2N_{\text{S\&C}})$), also as discussed in [6].

2) Preamble Blocks for Tsai Algorithm: In [7], multiple pairs of preamble OFDM symbols are used to estimate the SFO via weighted least-squares estimation and enable its correction with a resampling algorithm. In all these pairs, the second OFDM symbol in the discrete-frequency domain is equal to the multiplication of first by a known PRBS. In the considered PMCW-based RadCom system, however, changing the spectral content of a LFSR-generated PRBS is not possible. Instead, pairs of identical PRBSs are used. To avoid the need for extra shift registers, these are chosen to be identical to

the one that is later modulated and repeated in the PL. The use of identical pairs of identical PRBSs implies in the fact that no CP is needed between the aforementioned PRBS pairs. Therefore, a single copy of the adopted PRBS is prepended to the following PRBSs pairs to act as CP and avoid interblock interference from the previously transmitted S&C preamble blocks, which results in an odd total number of used PRBSs used for SFO estimation M_{SFO}.

Based on the proposed preamble design, one can conclude that a total of three LFSRs are needed in the considered PMCW-based RadCom system: two to generate $N_{\mathrm{S\&C}}$-length PRBSs for the S&C algorithm, and one to generate the N-length PRBS used for both the Tsai algorithm and the PL.

B. Block Pilot Arrangement

A set of PL blocks spaced by $\Delta M_{\mathrm{pil}} \in \mathbb{N}_{>0}$ blocks in the transmit PMCW frame is reserved as depicted in Fig. 2 and converted into pilot blocks by setting the BPSK symbol that modulates than to 1. Assuming that the pilot arrangement is known at the receiver, these blocks are accumulated and further processed to yield channel estimates for equalization and estimation and correction of the Doppler shift at the main path. The use of entire blocks with a block spacing of ΔM_{pil} enables estimating channel responses with a maximum delay

$$\tau_{\mathrm{max}} = N/F_{\mathrm{s}}, \tag{2}$$

and a maximum absolute Doppler shift at the main path [4]

$$f_{\mathrm{D,max}} = [2(NA/F_{\mathrm{s}})\Delta M_{\mathrm{pil}}]^{-1}. \tag{3}$$

Since even slight biases of the SFO estimate with the Tsai algorithm result in performance degradation due to the accumulation of the SFO effect over a high number of blocks, the obtained channel impulse response (CIR) estimates with pilots can also be used to calculate and correct the residual SFO. This is achieved by compensating the linearly increasing delay along the blocks caused by the residual SFO [8].

IV. MEASUREMENT SETUP AND RESULTS

In this section, proof-of-concept measurements are presented to validate the proposed PMCW-based RadCom system. In this context, a setup consisting of two Zynq UltraScale+ RFSoC ZCU111 system-on-a-chip (SoC) platforms from Xilinx, Inc, was adopted. While the first ZCU111 emulated the transmitter of a PMCW-based RadCom system, the second ZCU 111 acted as the receiver for another PMCW-based RadCom system, both with $F_{\mathrm{s}} = 1\,\mathrm{GHz}$. The DACs of the transmitter board were directly connected to the analog-to-digital converters (ADCs) of the receiver board via coaxial cables. Since the transfer functions of DACs, ADCs, and cables were not calibrated, a channel with a main, stronger line-of-sight (LoS) path and more severely attenuated secondary paths between transmitter and receiver was emulated at an intermediate frequency (IF) of $1\,\mathrm{GHz}$. Despite the fact that radio-frequency (RF) AFEs were not used, STO, CFO, and SFO could be experienced as the transmitter and receiver boards had distinct time, frequency, and sampling clock references.
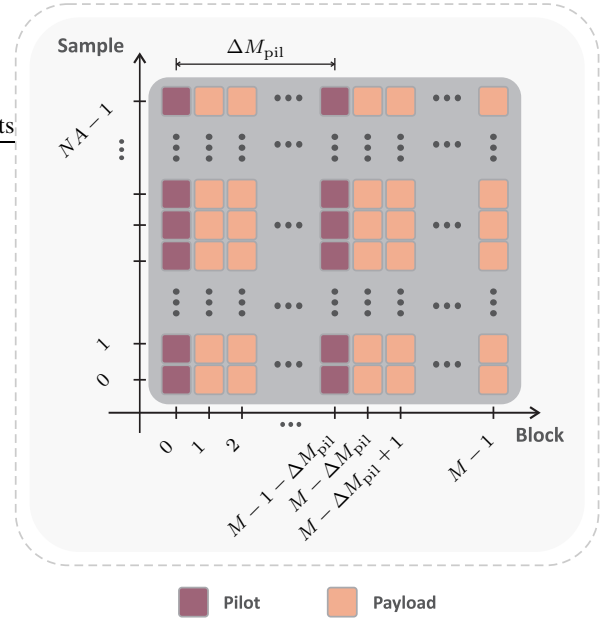

Fig. 2. Structure of the transmit PMCW frame containing PL and pilots in the discrete-time domain. For simplicity, the preamble is ommited.

A total of four distinct parameterizations, henceforth referred to as PMCW #1 to #4, were adopted for the PMCW-based RadCom system aiming HAD applications. All of them were defined seeking to achieve roughly the same dwell time of approximately $10.50\,\mathrm{ms}$ for the PMCW frame including preamble. The considered RF parameters, PMCW signal parameters, and the resulting communication and radar performance parameters, the latter calculated based on [3], [5], are listed in Table I. For conciseness, parameters that can be derived from already listed ones have been omitted. Additionally, the emulated carrier frequency of $79\,\mathrm{GHz}$ was only used to define the Doppler shifts that would result in the calculated radar velocity resolution and unambiguity. Since no additional Doppler shift to the CFO was added in the measurements, the pilots were rather used to estimate a residual CFO after correction with the S&C algorithm. The results from Table I show that, keeping A and increasing N yields higher communication processing gain $G_{\mathrm{p,comm}} = (N(A-1))$ and maximum delay for communication, while both the maximum Doppler shift and the data rate decrease due to the longer block duration. Similarly, radar maximum unambiguous range and velocity increase and decrease, respectively, along with N.

Finally, multiple measurements for PMCW #1 to #4 were performed with an signal-to-noise ratio (SNR) of around $16.23\,\mathrm{dB}$. The achieved mean and standard deviation of the estimated synchronization mismatches in Table II show that the precision of CFO and SFO estimates with the S&C and Tsai algorithms, respectively, increases with N and $N_{\mathrm{S\&C}}$, i.e., from PMCW #1 to #4, which agrees with [6] and [7]. The changes in the mean values are explained by the drift of time, frequency and sampling references during the measurements. Regarding residual CFO estimates with pilots, PMCW #1 to

TABLE I: PMCW-based RadCom system parameters.

	PMCW #1	PMCW #2	PMCW #3	PMCW #4
PMCW signal parameters				
Emulated carrier freq. (f_c)	79 GHz			
Sampling frequency (F_s)	1 GHz			
PRBS length (N)	255	511	1023	2047
PRBS repetitions for acc. (A)	5			
PL and pilot blocks (M)	8192	4096	2048	1024
S&C PRBS length ($N_{S\&C}$)	127	255	511	1023
PRBS for SFO est. (M_{SFO})	21			
Pilot block spacing (ΔM_{pil})	5			
Communication performance parameters				
Comm. process. gain ($G_{p,comm}$)	30.09 dB	33.10 dB	36.12 dB	39.13 dB
Maximum delay (τ_{max})	0.26 μs	0.51 μs	1.02 μs	2.05 μs
Max. Doppler shift ($f_{D,max}$)	78.43 kHz	39.14 kHz	19.55 kHz	9.77 kHz
Data rate (100% duty cycle)	627.03 kbit/s	312.67 kbit/s	156.00 kbit/s	77.78 kbit/s
Radar performance parameters				
Radar process. gain ($G_{p,rad}$)	69.22 dB	69.23 dB	69.23 dB	69.23 dB
Range resolution (ΔR)	0.15 m			
Max. unamb. range ($R_{max,ua}$)	38.22 m	76.60 m	153.34 m	306.84 m
Velocity resolution (Δv)	0.18 m/s			
Max. unamb. velocity ($v_{max,ua}$)	744.09 m/s	371.32 m/s	185.48 m/s	92.69 m/s

TABLE II: Synchronization performance results. Mean value and standard deviation of estimated parameters over multiple measurements are shown.

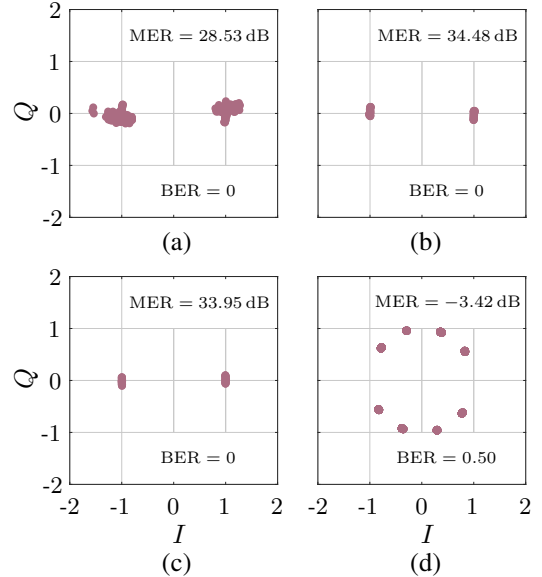|	PMCW #1	PMCW #2	PMCW #3	PMCW #4
CFO via S&C (kHz)	-83.76 ± 7.84	-84.93 ± 6.11	-85.26 ± 1.17	-86.20 ± 0.92
Resid. CFO via pilots (kHz)	-15.62 ± 8.14	-15 ± 6.31	-15.01 ± 1.31	5.86 ± 0.80
SFO via Tsai (ppm)	98.38 ± 5.98	99.62 ± 1.76	100.28 ± 0.91	99.63 ± 0.19

Fig. 3. Superimposed normalized receive BPSK constellations from all measurement realizations for (a) PMCW #1, (b) #2, (c) #3, and (d) #4.

#3 achieved sufficient accuracy, while PMCW #4 estimated a strongly biased residual CFO, i.e., 5.86 kHz instead of around -15 kHz, due to its constraining to ±9.77 kHz. Next, Fig. 3 shows the superimposed normalized receive BPSK constellations from the all measurements and their corresponding modulation error ratio (MER) and bit error ratio (BER) values. Although the obtained MERs are not equal to the input SNR plus the expected $G_{p,comm}$, which is in part due to imperfections in synchronization and channel estimation, a tendency of increasing MER along with $G_{p,comm}$ is observed from PMCW #1 to #2. Between PMCW #2 and #3, the MER slightly decreases mainly due to the accumulated effect of residual CFO and SFO between largely spaced pilots even after dual compensation, which degrades the quality of the obtained channel matrix used for equalization. Finally, a negative MER was achieved by PMCW #4 due to its ambiguous residual CFO estimate, which led to rotations of the obtained constellations w.r.t. the expected ones and resulted in a BER of 0.50.

V. CONCLUSION

This article introduced a strategy for synchronization and channel estimation in radar-centric PMCW-based RadCom systems based on PRBSs generated by LFSRs. In this context, the design of compatible preambles with the S&C and Tsai algorithms typically used for time, frequency and sampling frequency synchronization in OFDM, and the arrangement of pilots for channel, Doppler shift, and residual SFO estimation were discussed. Finally, proof-of-concept measurements validated the proposed strategy, showing that a PMCW-based RadCom system achieves robust communication performance if correctly parameterized and same sensing performance to an equally-parameterized PMCW-based radar system.

ACKNOWLEDGMENT

REFERENCES

[1] L. Giroto de Oliveira et al., "Doppler shift tolerance of typical pseudo-random binary sequences in PMCW radar," *Sensors*, vol. 22, no. 9, pp. 1–21, Apr. 2022.

[2] F. Probst, A. Engelmann, P. Hetterle, V. Issakov, R. Weigel, and M. Dietz, "A 15-Gb/s PMCW radar PRBS-generator for MIMO and joint radar-communication systems," in *2022 Asia-Pacific Microw. Conf.*, 2022, pp. 288–290.

[3] L. Giroto de Oliveira, B. Nuss, M. B. Alabd, A. Diewald, M. Pauli, and T. Zwick, "Joint radar-communication systems: Modulation schemes and system design," *IEEE Trans. Microw. Theory Tech.*, vol. 70, no. 3, pp. 1521–1551, Mar. 2022.

[4] Y. L. Sit, B. Nuss, and T. Zwick, "On mutual interference cancellation in a MIMO OFDM multiuser radar-communication network," *IEEE Trans. Veh. Technol.*, vol. 67, no. 4, pp. 3339–3348, Dec. 2018.

[5] L. Giroto de Oliveira et al., "Doppler shift tolerance of accumulation and outer coding in MIMO-PMCW radar," *IEEE Microw. Wireless Compon. Lett.*, vol. 32, no. 3, pp. 257–260, Mar. 2021.

[6] T. M. Schmidl and D. C. Cox, "Robust frequency and timing synchronization for OFDM," *IEEE Trans. Commun.*, vol. 45, no. 12, pp. 1613–1621, Dec. 1997.

[7] P.-Y. Tsai, H.-Y. Kang, and T.-D. Chiueh, "Joint weighted least-squares estimation of carrier-frequency offset and timing offset for OFDM systems over multipath fading channels," *IEEE Trans. Veh. Technol.*, vol. 54, no. 1, pp. 211–223, 2005.

[8] F. Burmeister, R. Jacob, A. Traßl, N. Schwarzenberg, and G. Fettweis, "Dealing with fractional sampling time offsets for unsynchronized mobile channel measurements," *IEEE Wireless Commun. Lett*, vol. 10, no. 12, pp. 2781–2785, Dec. 2021.